8-29-2007

Physical Properties and Composition Effects on the Reactivity of Calcium-Based Sulfur Sorbents

D. J. Hasler
Iowa State University

Thomas D. Wheelock
Iowa State University, wheel@iastate.edu

L. K. Doraiswamy
Iowa State University

Kristen P. Constant
Iowa State University, constant@iastate.edu

Physical Properties and Composition Effects on the Reactivity of Calcium-Based Sulfur Sorbents

Abstract
A detailed comparison between agglomerated pellets of limestone and commercial-grade plaster of Paris was conducted to test the reactivity of the pellets with H2S over three cycles of sulfidation and regeneration. After multicycle testing with 1 vol % H2S at 880 °C, it was determined that the higher surface area exhibited by the plaster of Paris pellets provided a consistently higher reactivity than the limestone pellets. The effects of pore-forming additives on agglomerated limestone pellets was tested with starch, graphite, and poly(vinyl alcohol) (PVA). The results indicated that the PVA–limestone pellets exhibited a higher capacity for sulfur than plain limestone pellets over multiple cycles. A comparison between pellets made of two different grades of plaster of Paris, limestone, calcium carbonate, dolomite, and hydrated dolomite over three cycles of sulfidation and regeneration provided results indicating that plaster of Paris and hydrated dolomite exhibited the best reactivity and thermal stability. The plaster of Paris and hydrated dolomite also exhibited a capacity for H2S over eight cycles of sulfidation and regeneration that proved promising for possible application in IGCC systems.

Keywords
Chemical and Biological Engineering

Disciplines
Chemical Engineering | Materials Science and Engineering

Comments
Reprinted with permission from *Industrial & Engineering Chemistry Research* 46 (2007): 5913–5921, doi:10.1021/ie061561n.

Physical Properties and Composition Effects on the Reactivity of Calcium-Based Sulfur Sorbents

D. J. Hasler,*,†,‡ T. D. Wheelock,† L. K. Doraiswamy,† and K. P. Constant§

Department of Chemical Engineering and Department of Materials Science and Engineering, Iowa State University, Ames, Iowa 50011-2230

A detailed comparison between agglomerated pellets of limestone and commercial-grade plaster of Paris was conducted to test the reactivity of the pellets with H_2S over three cycles of sulfidation and regeneration. After multicycle testing with 1 vol % H_2S at 880 °C, it was determined that the higher surface area exhibited by the plaster of Paris pellets provided a consistently higher reactivity than the limestone pellets. The effects of pore-forming additives on agglomerated limestone pellets was tested with starch, graphite, and poly(vinyl alcohol) (PVA). The results indicated that the PVA−limestone pellets exhibited a higher capacity for sulfur than plain limestone pellets over multiple cycles. A comparison between pellets made of two different grades of plaster of Paris, limestone, calcium carbonate, dolomite, and hydrated dolomite over three cycles of sulfidation and regeneration provided results indicating that plaster of Paris and hydrated dolomite exhibited the best reactivity and thermal stability. The plaster of Paris and hydrated dolomite also exhibited a capacity for H_2S over eight cycles of sulfidation and regeneration that proved promising for possible application in IGCC systems.

Introduction

The innovation of more advanced materials over recent decades has resulted in more efficient, electrical energy systems. These new materials have enabled higher temperatures and pressures to be attainable in modern power plants, which have opened up new approaches to better utilize coal as a resource for energy. Although biorenewables offer a promising source of potential energy, fossil fuels will still be a primary energy source for most countries in the 21st century. Of the various fossil fuels, coal is one resource that is located in large quantities throughout the United States and the world. Since fossil fuels are a finite resource, more efficient systems must be implemented to maximize our use of such a plentiful and readily available resource. Systems such as the integrated gasification combined cycle (IGCC) can pave the way for more clean and efficient energy production by utilizing coal.

The IGCC system is based upon a process that first converts solid coal particles into a gas by a high-temperature, steam reforming reaction. The gas products are H_2 and CO.

$$C_{(s)} + H_2O_{(g)} \rightarrow H_{2(g)} + CO_{(g)} \quad (1)$$

Following the gasification processs, the H_2 and CO are combusted in a gas turbine and the excess heat from the exhaust is used to generate steam and power a steam turbine. During the gasification process, any sulfur present in the coal is converted to H_2S and COS and any trace amounts of metals are vaporized. The sulfur, vaporized metals, and entrained particles must be removed prior to introduction to the gas turbine. Typical gasifiers operate with gas outlet temperatures in the range of 800−1400 °C; therefore, in order to remove the sulfur species, either the gas must be cooled to a temperature suitable for wet chemical gas scrubbing or a solid sorbent is used to remove the sulfur through a gas−solid reaction. Since the efficiency of the IGCC system is directly related to the temperature of the incoming combustible gases prior to the gas turbine, it is advantageous to remove the sulfur at the highest possible temperature. Currently, materials such as Zn and Cu oxides are being tested in pilot plants for sulfur removal in the approximate range of 400−600 °C. Unfortunately, this temperature range requires the hot gases to be cooled, which reduces the overall efficiency of the IGCC system. Also, since the U.S. government's current energy plan, Vision 21,[1] states the need for coal-based energy systems to produce electricity with >60% efficiency by 2010, a high-temperature sulfur sorbent will eventually be needed.

If a solid oxide sorbent is to be used that can operate at high temperature and under severe reducing conditions, the most stable materials known to be available are the three primary oxides of Mn, Ce, and Ca.[2,3] Of these three compounds, CaO is the most stable at high temperatures, does not require pre-reduction prior to reaction with H_2S, and is the cheapest from the standpoint of mass production. Calcium oxide originally in the form of limestone or dolomite has been used successfully for a number of years as a solid oxide sorbent for SO_2 capture in fluidized bed combusters. Typically, the material is reacted and then discarded as $CaSO_4$, but CaO can also be used as an effective sorbent for removing H_2S and COS from gasified coal.

$$CaO_{(s)} + H_2S_{(g)} \rightarrow CaS_{(s)} + H_2O_{(g)} \quad (2)$$

$$CaO_{(s)} + COS_{(g)} \rightarrow CaS_{(s)} + CO_{2(g)} \quad (3)$$

Both H_2S and COS react readily with CaO at high temperatures (∼900 °C), making it a suitable solid oxide sorbent for high-temperature uses.

In addition to CaO exhibiting a high reactivity for H_2S, it can also be regenerated from its sulfided form by a cyclic oxidation and reduction process developed by Jagtap

* To whom correspondence should be addressed. Tel.: (515) 294-1660. Fax: (515) 294-2689. E-mail: david.j.hasler@sargentlundy.com, lkedson@iastate.edu.

† Department of Chemical Engineering.

‡ Present address: Sargent & Lundy LLC, 55 E. Monroe, Chicago, IL 60603.

§ Department of Materials Science and Engineering.

10.1021/ie061561n CCC: $37.00
Published on Web 08/02/2007

and Wheelock[4] that enables the conversion of CaS to CaO to take place very rapidly and efficiently at 1050 °C.

$$CaS_{(s)} + 2O_{2(g)} \rightarrow CaSO_{4(s)} \quad (4)$$

$$CaSO_{4(s)} + H_{2(g)} \rightarrow CaO_{(s)} + SO_{2(g)} + H_2O_{(g)} \quad (5)$$

The process can utilize air as the oxidant and the reducing gas can be H_2, CO, methane, ethane, or propane. The regeneration process has led to the potential use of CaO as a reusable H_2S and COS sorbent. A unique technique that adds structural integrity consists of combining a pelletized core of CaO with a strong and inert shell.[5]

Sintering has proven to be a reaction-inhibiting phenomenon for most materials at high temperatures regarding gas−solid or catalytic reactions. Since the reactivity of CaO with H_2S and COS is highly surface area dependent,[6−8] any sintering of the material leads to a decrease in capacity over multiple cycles of sulfidation and regeneration.[9] It is well documented that not only temperature but also H_2O and CO_2 combine to catalyze the sintering of CaO at high temperatures.[10−14] Therefore, a deterrent is sought that can hinder the sintering rate of CaO during multiple cycle operation with gasified coal.

In order to alter the rate of sintering of potential sulfur sorbents, the basic fundamentals must be understood. Sintering is a phenomenon by which mass transfer occurs to reduce the surface energy of a material. Areas of high surface energy can occur due to gas−solid chemical reactions, formation of liquid phases, irregular surface geometry (nonspherical), and particle−particle contact. In agglomerated pellets such as limestone or dolomite, particle−particle contact alone induces sintering due to surface tensions between the boundaries of particles. The result is neck growth between the particles, which eventually reduces the surface area of the material. Either coarsening, which is manifested in surface area loss only, or densification can compete depending upon the material and conditions.[15,16] The actual cause of sintering is quite complex when considering nonspherical particle geometry, nonuniform particle packing, and gas−solid, exothermic reactions taking place such as the reaction between calcium oxide and hydrogen sulfide or the regeneration of calcium sulfide. Some sintering inhibitors can be generalized as chemical constituents that retard solid-state ionic diffusion or grain boundary mobility, high pore coordination numbers within domains and agglomerates,[15] and increased porosity. All of these inhibitors can be utilized when designing a solid sulfur sorbent for use at high temperatures.

This paper discusses the results obtained while comparing the reactivity of a number of CaO-based materials with H_2S. The primary comparison was between a commercial-grade plaster of Paris and a pure form of limestone. The comparison was based upon physical measurements of the pellets' porosity, pore size distribution, surface area, apparent density, and sulfur reactivity over a number of stages of processing and high-temperature gas−solid reactions. In addition, some preliminary work with three different types of pore-forming additives incorporated into agglomerated limestone pellets is also presented and discussed. Results from sulfidation tests with different forms of dolomite, plaster of Paris, and $CaCO_3$ are presented for comparison, along with eight cycle sulfidation/regeneration tests of two promising sulfur sorbent materials.

Experimental Section

The first form of plaster of Paris was obtained from United States Gypsum Oklahoma (POP1), while the second was from DAP, Inc. (POP2). The dolomite and dolime, which is a hydrated form of dolomite, were from Graymont Dolime (OH), Inc. The limestone was obtained from the Martin Marrietta quarry of Ames, IA, and the reagent-grade calcium carbonate was from Fisher Chemicals.

All the reactions were carried out in a high-temperature, tubular reactor. The reaction progress was monitored using a Cahn 2000 TGA connected to a PC for data acquisition. The TGA was used to monitor the weight changes of the reacting materials. The pellets were suspended in a quartz basket that was vertically suspended by quartz hang-down wires in the center of a 2.5 cm i.d. quartz tube. The quartz tube had an overall length of 61 cm, of which 30.5 cm was heated by a high-temperature box furnace. A thermocouple inside a quartz thermowell was placed directly below the sample basket in the center of the heated section of the tube. The gas flow rates were held constant at 500 mL/min for both sulfidation and regeneration reactions. All sulfidation reactions were carried out at 880 °C with 1 vol % H_2S and 24 vol % H_2 in N_2. The sulfur capacity was calculated based upon the overall pellet weight including any inert material (eq 6).

$$\text{sulfur capacity (\%)} = \frac{\text{wt}_{(\text{CaO+CaS+inert})} - \text{wt}_{(\text{CaO+inert})}}{\text{wt}_{(\text{CaO+inert})}} \times 100 \quad (6)$$

The regeneration reactions were carried out at 1050 °C using 13 vol % O_2 in N_2 and 9 vol % H_2 in N_2.

The pellets were tested in spherical, pellet form, which were approximately 3.5 mm in diameter. The dolomite, dolime, limestone, and $CaCO_3$ materials were pelletized in a bench-scale pelletizer with a binder composed of a dilute solution of lignin in deionized water. The plaster of Paris pellets were made in the same pelletizer as the limestone pellets, but deionized water was used as the binder. The pellets made with pore-forming additives were initially wet-mixed as slurry in a solution of deionized water and 1 wt % sodium hexametaphosphate. After the slurry was mixed for 30 min at 120 rpm with a commercial liquid mixer, it was dried at 110 °C and ground with a mortar and pestle. The powder was then pelletized, utilizing a dilute solution of lignin in deionized water.

The surface area measurements and pore size distribution were measured using a Micromeretics ASAP 2000 surface area analyzer with N_2 as the adsorbent. Multiple measurements were taken and averaged for each data point, and each sample consisted of approximately 20 pellets. The apparent density and total open pore porosity was obtained by applying Archimedes' principle. All measurements were carried out by first placing approximately 5 pellets in a glass beaker within a desiccator to which was applied a vacuum to remove the air from the pores. After ∼1 h, and while the system was still under vacuum, *n*-decane was introduced through a custom funnel which allowed the *n*-decane to fill the beaker and completely cover the pellets. The desiccator was then slowly pressurized to ambient conditions, which forced the *n*-decane into the open pores saturating the pellets. The pellets were left submerged in the *n*-decane for ∼1day before the apparent density and open pore porosity measurements were taken. Groups of five pellets were used for each measurement, and a total of three groups was averaged for each data point.

Results and Discussion

Limestone vs Plaster of Paris. The initial work was begun by comparing the reactivity of pelletized limestone and plaster

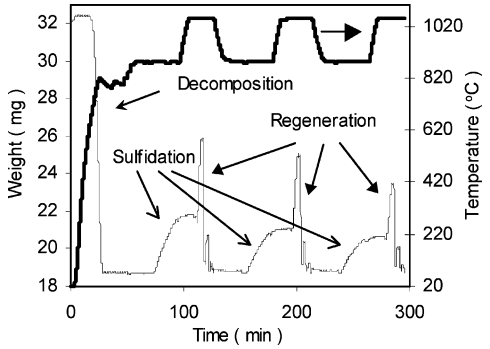

Figure 1. Limestone pellet calcined, sulfided, and regenerated through three consecutive cycles.

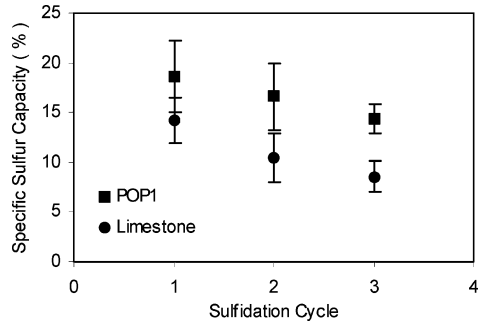

Figure 2. Specific sulfur capacity of pellets averaged over multiple cycles of sulfidation and regeneration (95% CI).

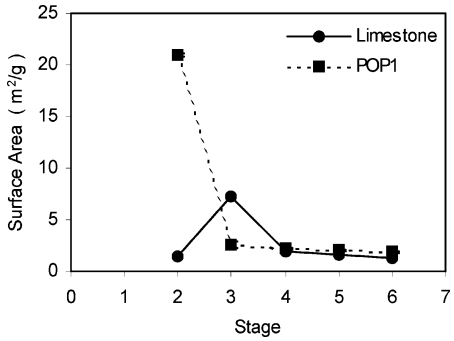

Figure 3. Specific surface area of the pellets measured throughout six different stages of processing and reaction (95% CI).

of Paris pellets with 1 vol % H_2S and 24 vol % H_2 in N_2 at 880 °C in the TGA reactor system. The H_2 was utilized to prevent the thermal decomposition of the H_2S and to simulate the reducing conditions present in gasified coal. Each sulfidation was carried out for 20 min followed by a temperature ramp to 1050 °C, at which temperature the regeneration was carried out using 9 vol % H_2 in N_2 for reduction and 13 vol % O_2 in N_2 for oxidation. An example of a complete run is shown in Figure 1. The regeneration typically lasted for 15 min and was carried out through four cycles. The results after the three cycles of sulfidation and regeneration are presented as specific sulfur capacity versus sulfidation cycle in Figure 2 for both types of pellets with 95% confidence intervals (CIs). Each data point represents an average of at least three single pellet tests. The comparison reveals the significant difference between the two types of pellets regarding the rate of decline of specific sulfur capacity, which was rather compelling considering the similar composition of the two materials (Table 1). Therefore, a study was undertaken to determine the reason for the higher stability of the POP1 pellets.

The study involved the physical characterization of the two types of pellets throughout six stages of processing and reaction

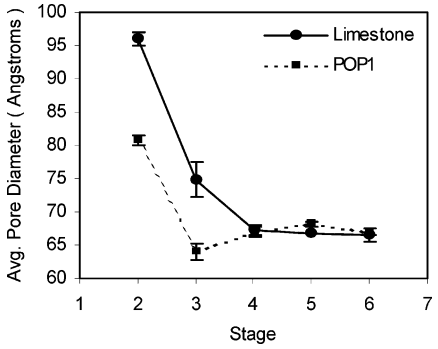

Figure 4. Average pore size of limestone and POP1 pellets in the 20−3700 Å range (95% CI).

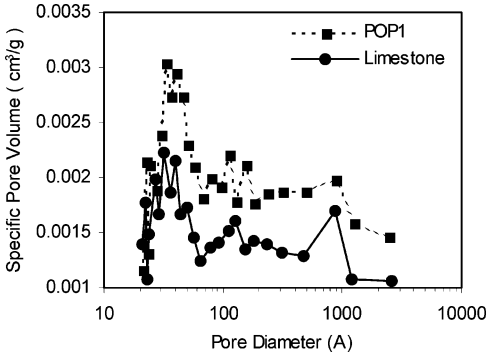

Figure 5. Pore size distribution of POP1 and limestone pellets at stage 6.

Table 1. Chemical Composition of Materials Used

component	POP1	POP2	limestone	$CaCO_3$	dolomite	dolime
$CaSO_4 \cdot {}^1/_2H_2O$	98	78				
$CaCO_3$		15	95.75	100		
$CaCO_3 \cdot MgCO_3$		6	1.77		97.9	97.1
$Ca(OH)_2 \cdot Mg(OH)_2$						
$MgCO_3$	0.16					
SiO_2	0.20		0.752		0.3	0.37
Al_2O_3			0.155			
Fe_2O_3			0.216			
$SrSO_4$	0.26					
$MgSO_4 \cdot 7H_2O$	0.19					
other	1.19	1	1.357		1.9	2.6

cycles. Stage 1 corresponds to the green agglomerated pellets post pelletization, stage 2 corresponds to the pellets post heat treatment at 110 °C under vacuum, and stage 3 represents the limestone pellets after calcination at 880 °C (conversion of $CaCO_3$ to CaO) and the POP1 pellets after conversion from $CaSO_4$ to CaO at 1050 °C utilizing the cyclic reduction and oxidation process. Stage 4 represents post sulfidation and regeneration cycle 1 for the limestone and POP1 pellets. Stages 5 and 6 represent post sulfidation and regeneration cycles 2 and 3, respectively.

Since the reaction between CaO and H_2S has been determined to be surface area dependent, this parameter is compared first in Figure 3. The results indicate that upon heat treatment at 110 °C under vacuum, the surface area of the POP1 pellets rose considerably. The rise in surface area was due to the removal of the water of hydration, leaving a very porous structure. The POP1 powder began as $CaSO_4 \cdot {}^1/_2H_2O$, but during pelletization with deionized water it underwent hydration to form the dihydrate, $CaSO_4 \cdot 2H_2O$. The limestone did not undergo a chemical change during pelletization since the $CaCO_3$ is unreactive with the water-based solution used for agglomeration of the powder; therefore, no increase in surface area resulted after the residual moisture was removed. Following the vacuum and low-temperature heat treatment, the POP1 pellets were

Table 2. Surface Area and Porosity Measurements for POP1 and Limestone Pellets after Multiple Stages of Processing and Sulfidation/Regeneration[a]

	POP1			Limestone		
		Porosity (cm^3/g)			Porosity (cm^3/g)	
stage	surface area, SA (m^2/g)	2 nm < D < 370 nm	D > 370 nm	surface area, SA (m^2/g)	2 nm< D < 370 nm	D > 370 nm
2	21 ± 1.0	0.0423	0.463	1.49 ± 0.019	0.0036	0.269
3	2.6 ± 0.3	0.0042	1.059	7.3 ± 0.2	0.0136	0.711
4	2.18 ± 0.09	0.0037	1.042	1.89 ± 0.06	0.00317	0.701
5	2.02 ± 0.04	0.00344	1.054	1.53 ± 0.016	0.00256	0.611
6	1.89 ± 0.06	0.00316	1.015	1.36 ± 0.07	0.00227	0.599

[a] Surface areas include 95% CI.

converted to CaO at 1050 °C by the cyclic oxidation/reduction process and the limestone pellets were converted to CaO through the endothermic decomposition/calcination of $CaCO_3$ during the temperature ramp to 880 °C.

After the initial conversion process the specific surface area of the two materials was reversed. The limestone pellets became more porous and subsequently a higher surface area was evolved due to the loss of CO_2, while the POP1 pellets underwent a significant loss in surface area. It was assumed that the POP1 pellets would also become more porous due to the removal of SO_3 from within the structure of the pellets, and would remain more porous than the limestone pellets since the crystal density of $CaSO_4 \cdot 2H_2O$ is 2.32 g/cm^3 versus that of $CaCO_3$, which is 2.872 g/cm^3. Apparently, the transformation of the POP1 pellets from $CaSO_4$ to CaO, and the time of exposure at 1050 °C during the high-temperature oxidation/reduction cycle, sintered the material to such an extent as to remove any extra surface area that might have been evolved. Because the limestone pellets had a higher surface area than the POP1 pellets prior to the first sulfidation run, they should have yielded a higher rate of reactivity, which was not the case. Since sintering is a function of temperature and time of exposure, if the limestone pellets were sintering at a more rapid pace than the POP1 pellets, it was only a matter of time or sulfidation/regeneration cycle before the surface area of the limestone pellets dropped below that of the POP1 pellets. The surface area measurements at stage 4 revealed such a case when the POP1 pellets exhibited a higher value. The fourth-stage surface area values help to support the idea that sometime during the first sulfidation cycle the surface area of the limestone pellets actually dropped below that of the POP1 pellets, which lowered its sulfur capacity in comparison to the POP1 pellets. The POP1 pellets continued to exhibit a surface area higher than the limestone pellets throughout stages 5 and 6 with the difference becoming more pronounced. A closer look at the surface area measurements of the two materials throughout stages 4−6 in Table 2 reveals that they are quite different quantitatively. In fact, the limestone pellets exhibited a surface area that was 13%, 24%, and 28% lower than that of the POP1 pellets throughout stages 4, 5, and 6, respectively.

Following the surface area comparison, the pellets were examined for their average pore size in the diameter range of 20−3700 Å. The measurements revealed that the average pore diameters of the pellets were quite similar from stages 2 to 6 (Figure 4). The only significant difference was the higher average pore diameter exhibited by the limestone pellets during the second and third stages. An intriguing aspect of the results is the similar values once the sulfidation/regeneration cycles began (stages 4−6), especially when regarding the chemical composition of the starting materials ($CaSO_4$ vs $CaCO_3$). It is possible that the pelletization process, in conjunction with the particle size of the starting materials, provided a structural pore network that was similar and only became pronounced once both materials were converted to CaO and severe sintering had occurred.

Because the average pore diameters of both types of pellets were so similar throughout stages 4−6, the pore size distribution of the pellets was examined to see if there were any substantial differences. The distribution of the apparent pore sizes was compared in Figure 5 for both types of pellets after the final sulfidation and regeneration cycle (stage 6). The measurements indicated that both materials exhibited a substantial population of pores in the 25−50 Å range. On a comparison basis, the only significant difference between the two materials based upon these measurements was the larger number of pores per diameter exhibited by the POP1 pellets. Because the pore size distributions were so similar, the calculated effective diffusivity was the same. Therefore, it is probable that both types of pellets exhibited similar rates of gas-phase diffusion within the pores, unless there was a large difference in tortuosity. The tortuosity was not measured nor estimated for either of the two materials.

The apparent density of the materials was measured throughout the six stages to investigate whether one material was densifying at a more rapid rate. (See Figure 6.) The first four stages showed a progression toward a more dense material state that reached a maximum for both materials by stage 4. At stage 4, the materials exhibited densities that were similar to that for the pure form of CaO, which is in the range of 3.3−3.7 $g/cm.^3$ The following stages (5 and 6) resulted in decreases in both materials' density. Generally, such a phenomenon can occur during the densification of ceramic materials and can be the result of a decrease in the rate of densification and an increase in coarsening effects. In general, both materials appeared to follow the same rate of densification throughout all six stages. A more quantitative comparison would be warranted if it were not for the error in the measurements.

The total open pore porosity of the pellets was compared which revealed that both pellets increased in porosity at a similar rate through stages 1−4, but deviated in stages 5 and 6. The most distinguishable difference between the two materials, aside from the POP1 pellets' higher porosity throughout all six stages, was in stages 5 and 6 where the POP1 pellets' porosity remained steady while the limestone pellets' dropped in value (Figure 7). While it is difficult to postulate at this time why the two materials exhibited such different trends in stages 5 and 6, some comparisons can be made regarding diffusivity effects. Because the POP1 pellets contained a higher macroporosity (Table 2), it is possible that this enhanced the rate of diffusion within the pellets and subsequently had an effect on the rate of reaction. However, the data in Table 2 show that between stages 4 and 6 the macroporosity (pore diameter >370 nm) of the POP1 pellets increased (stage 5), while the sulfur capacity continued to decrease. These contrasting results indicate that

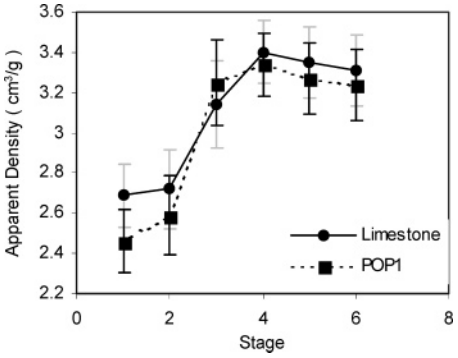

Figure 6. Apparent density of the pellets versus number of processing and reaction stage (95% CI).

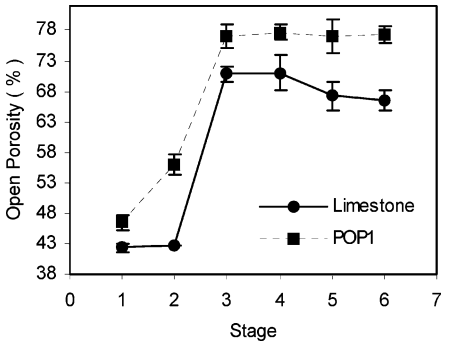

Figure 7. Open pore porosity of the pellets throughout the stages of processing and reaction (95% CI).

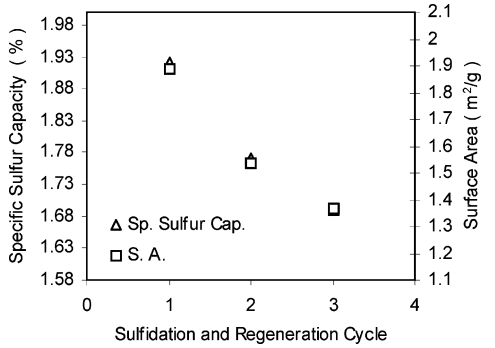

Figure 8. Comparison between specific sulfur capacity and surface area of limestone pellets as a function of consecutive sulfidation/regeneration cycles. Pellets tested in groups of 10.

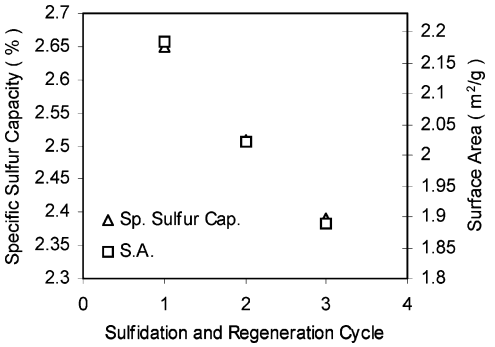

Figure 9. Comparison between specific sulfur capacity and surface area of POP1 pellets as a function of consecutive sulfidation/regeneration cycles. Pellets tested in groups of 10.

any apparent increase in mass transfer caused by the increasing macroporosity of the POP1 pellets was negated by a more dominant material effect resulting in the decreasing sulfur capacity (Figure 2). Therefore, the total open pore porosity results indicate that diffusivity was probably not the dominating mechanism to differentiate between the two materials' diverse, declining sulfur capacities.

Following the macroporosity, the meso−macroporosity (pore diameter $2 < D < 370$ nm) values for both types of pellets were compared. The results show that, throughout stages 4−6, the mesoporosity values appeared to decline at a similar rate as the surface area for both types of pellets. The relation between the declining rate of the meso range of pores and the surface area is due to the large surface area inherent in the meso range of pores for these two materials. The loss in total surface area is due to particle coalescence during the sintering of the domains (interparticle pores), which eliminates pores in the meso range.

Since the average pore size of the pellets decreased at a rate similar to the sulfur capacity of the pellets over stages 4−6, a qualitative comparison was made between the sulfur capacity and the surface area for stages 4−6 as shown in Figures 8 and 9. The comparison revealed the significant correlation between the sulfur capacity and surface area of the two types of pellets throughout the three sulfidation/regeneration stages. The reason for the low, specific sulfur capacity values exhibited by both types of pellets in Figures 8 and 9 was a result of testing ~20 pellets in the reactor at the same time for a reaction time of only 30 min, with 1.0 vol % H_2S. A large sample size was used for sulfidation testing to increase the accuracy of the surface area analysis.

In order to gain some insight into the difference in sintering rates, the rate of surface area loss as a function of sulfidation/regeneration cycle was fitted with a basic, two-parameter, power law function (eq 7):

$$\frac{\mathrm{d}}{\mathrm{d}t}\left(\frac{S}{S_o}\right) = k\left(\frac{S}{S_o}\right)^n \tag{7}$$

The power law function is commonly employed empirically to account for sintering and deactivation of heterogeneous catalysts.[17,18] The data indicated that the limestone and POP1 pellets' rate of surface area loss was suitably fitted with eq 7 by using the sulfidation/regeneration cycles as the independent variable (t). The data fitting results yielded an exponential value of $n = 3$, rate constant of $k = 0.1677$, and correlation coefficient of $R^2 = 1$ for the POP1 pellets and $n = 5$, $k = 1.3305$, and $R^2 = 0.9997$ for the limestone pellets. Typical values of n can range from 2 to 16,[17,18] when studying the initial rate of sintering. Because these particular studies were conducted throughout different process stages that involved changing temperatures and relatively long amounts of time between surface area measurements, the values of n and k represent the latter stages of sintering. The pronounced differences in the rates of sintering are apparent both in the linear constant, k, and in the exponential constant, n. The significant differences suggest alternate mechanisms of mass transport leading to coarsening and densification.

Whereas the rate of surface area loss was significantly higher for the limestone pellets, both pellets exhibited an interesting relationship when comparing the specific sulfur capacity to surface area as shown in Figure 10. Once the surface area reached a value of ~2 m^2/g for both materials, the values of each specific sulfur capacity coincided. Because the reaction is of gas−solid nature, once the available calcium oxide surface sites are converted to the sulfide form the O^{2-} and S^{2-} ions

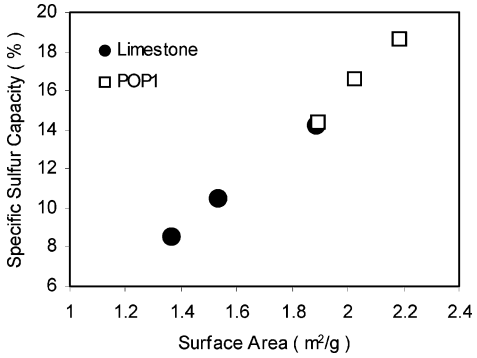

Figure 10. Comparison between specific sulfur capacity and surface area for limestone and POP1 pellets. Data taken from three consecutive sulfidation/regeneration cycles.

must counterdiffuse in the solid state to convert the inner calcium oxide. Therefore, a high surface area sulfur sorbent will have a high, initial reaction rate, and also enable a higher flux of ions to facilitate the solid-state reaction. If the reticulated structure that makes up the different pellets is similar in thickness, then the specific sulfur capacities should be very similar if the pellets are compared when they exhibit the same specific surface area.

The experimental results indicate that surface area was the primary physical factor causing the difference in reactivity between the limestone and POP1 pellets. As stated previously, the surface area of CaO has been reported to be the primary physical parameter that determined the rate of reaction between H_2S and CaO.[6−8] Since both forms of CaO tested were of relatively pure composition, the effect of the starting material's physical structure in the pelletized form probably played a significant role in the overall effectiveness of the pellets. The findings further justify efforts to develop more porous structures that not only improve the reactivity through increased surface area, but also prevent or hinder the rate of sintering by reducing particle−particle contact within the pellets. The minor chemical constituents present in both starting materials presumably had an effect on the pellets, but it is assumed that the effects were primarily surface area related (sintering) and not directly chemical. Further work needs to be conducted to address the effects from minor chemical impurities.

Pore-Forming Additives. The previous results showed that a more stable form of limestone or CaO-based sorbent needs to be developed to maintain the high initial sulfidation rate of CaO for multicycle industrial use. Since there are a number of approaches to be chosen from to limit the sintering rate, the simplest and least expensive is desired from a manufacturing standpoint. One of the most basic approaches to constrain the sintering of a material is to increase the number of micro and meso ranges of pores. A technique by which the porosity of an agglomerated pellet can be enhanced is conducted by simply incorporating an additive during the pelletization process that is later removed at high temperatures. The process of removing the additives from the pellets during the heating to reaction temperatures creates added porosity within the pellets and therefore reduces particle−particle contact, thereby constricting the driving force for sintering.

Since the spherical pellets were made by pelletization, a pore-forming additive that could be physically mixed with the powders prior to pelletization was chosen. Limestone was chosen as the precursor of CaO since it is found in large quantities in a relatively pure form, is currently used in industrial power plants for SO_2 removal, and is appealing from a large-scale-production standpoint. The materials were tested over

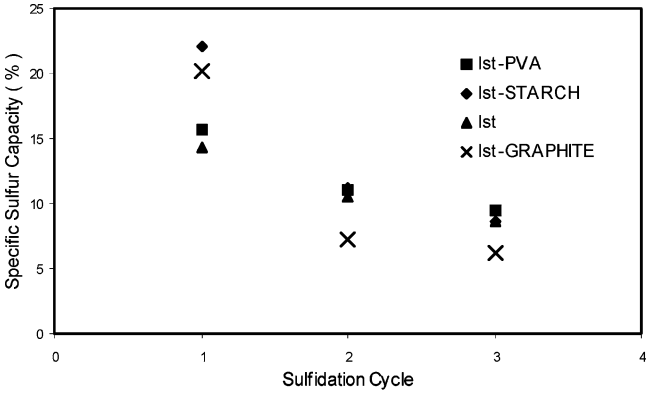

Figure 11. Effects of pore-forming additives on reactivity of limestone pellets over multiple cycles of sulfidation and regeneration.

Table 3. Specific Sulfur Capacity of Pellets with Pore-Forming Additives Measured throughout Three Stages of Sulfidation and Regeneration

sulfidation cycle	Specific Sulfur Capacity			
	limestone	lstPVA	lstGR	lstST
1	14.27	15.75	20.1	22.03
2	10.47	11.05	7.2	11.27
3	8.57	9.55	6.2	8.7

multiple cycles of sulfidation/regeneration with three different additives: starch, poly(vinyl alcohol) (PVA), and graphite. The first two materials were chosen due to their solubility in an aqueous environment and low decomposition temperatures. The graphite was chosen because of its stability at lower temperatures, thereby enabling an additional effect to be considered (pore formation at high temperatures). All three types of pellets were prepared as discussed in the Experimental Section. The limestone−starch (lstST) and limestone−PVA (lstPVA) pellets' pore-forming additives were removed via pyrolysis during heating to the sulfidation reaction temperature of 880 °C. The limestone−graphite (lstGR) pellets were preoxidized with a dilute O_2 stream during heating to remove the graphite prior to sulfidation.

The experiments were performed with at least three pellets of each type randomly chosen and tested individually, so an average could be computed for each composition. All of the pellets were reacted at 880 °C with 1.0 vol % H_2S and 24 vol % H_2 in N_2, and were regenerated with 9 vol % H_2 and 13 vol % O_2 in N_2 at 1050 °C. Three sulfidation/regeneration cycles were carried out for each type of pellet tested. The sulfidation runs were 20 min in length.

The comparison between the limestone pellets with and without pore-forming additives is shown in Figure 11 (the data are given in Table 3). Every type of pellet with a pore modifier revealed an increase in sulfur capacity above that of the plain limestone pellets during the first sulfidation cycle. The first cycle revealed very high capacities exhibited by the lstST and lstGR pellets that resulted in sulfur capacity improvements exceeding the plain limestone pellets by 5%, while the lstPVA pellets exhibited a more modest increase in capacity of approximately 1.5%. Following the first cycle, the lstPVA pellets continued to yield a sulfur capacity that was slightly higher than the plain limestone pellets through the second and third cycles. The sulfur capacity results for the lstGR pellets through the second and third cycles fell well below those of the plain limestone pellets.

Similar work with graphite as a pore-forming additive was carried out by Pineda and Palcios,[18] which involved extruded zinc titanate pellets mixed with different amounts of graphite and tested with H_2S in a fixed bed apparatus. The initial tests

indicated that the inclusion of graphite increased the sulfur capacity of zinc titanate, but subsequent cycles revealed a decrease in capacity with each sulfidation/regeneration cycle. Unlike the results with the lstGR pellets, the graphite−zinc titanate sorbents did not appear to exhibit a reactivity lower than that of plain zinc titanate. One aspect of using graphite that could have possibly led to an increase in sintering is the exothermic, partial oxidation reaction that took place. The heat from the exothermic reaction could have made the pellets more susceptible to sintering, which was only manifested in the cycles following the first initial sulfidation reaction. Such an effect could be due to unoxidized graphite that remained after the preoxidation step and before the first regeneration. The remaining graphite would have been oxidized during the regeneration cycle, which would have additionally increased the sintering effects. After further analysis it was discovered that a small weight change (<1 wt %) had occurred between the first and second sulfidation cycles for each of the lstGR pellets tested, indicating that some residual graphite was removed via oxidation during the first regeneration cycle. Since the O_2 concentration was much higher during the regeneration cycles, 20 vol %, the oxidation of the graphite probably occurred as full combustion versus partial oxidation, and therefore emitted a substantial amount of heat in the vicinity of the graphite particles.

The lstST pellets exhibited an improved sulfidation capacity through the first and second cycles, but by the third cycle the sulfur capacity had declined to the level of the limestone. The initial, high capacity of the lstST pellets was most likely due to an increase in exposed surface area (pellet cracks) that was visible well into the depths of the pellets. Because the cracks exposed more surface area to the reactant gases, the first cycle probably benefited the most, since rapid sintering likely reduced the pellets' surface area to a value that was comparable to the plain limestone, and therefore rendered the exposed surfaces less effective for the subsequent sulfidation cycles. The formation of the cracks in the pellets might have been caused by the rapid decomposition process and subsequent high rate of mass loss in concentrated sectors of the pellets. Such effects would be instigated by starch tending to flocculate during the pelletization process leading to the formation of large agglomerates within the pellets. An ineffective dispersion of the starch might have also occurred during the mixing of the slurry, resulting in the same effects. Since sodium hexametaphosphate (NaHMP) was utilized with all three pore forming additives, the effects from such an additive might have increased the rate of sintering. Therefore, if the NaHMP did affect the sintering rate, then the results represent only relative differences amongst the additives and their performance with regards to plain limestone could possibly improve.

The lstPVA pellets exhibited the most promising performance of all three types of pellets tested with an additive. The sulfur capacity of the lstPVA pellets remained higher than that of the plain limestone pellets throughout all three cycles. The improvement in capacity was very modest but remained constant and did not appear to decrease as rapidly as that of the limestone pellets. It is possible that the PVA was more homogeneously dispersed during the slurry and pelletization process than the starch or graphite. Because only one type of dispersion slurry was tested, the starch could possibly provide similar or better benefits than the PVA if adjustments were to be made to the slurry mixture.

Materials Comparison. An overall comparison of potential suflur sorbents was made between two types of plaster of Paris (POP), two types of dolomite, and two types of $CaCO_3$ for their reactivity with H_2S at 880 °C in agglomerated pellet form. The comparison was made by testing individual pellets in the reactor system for 20 min of sulfidation followed by regeneration. All conditions were the same as described earlier. The results from the comparisons are presented in Figure 12 (the data are given in Table 4).

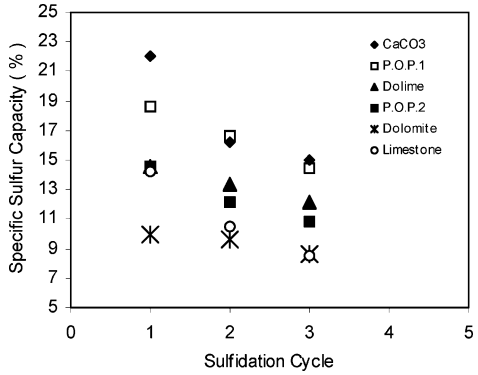

Figure 12. Comparison between multiple starting materials in pellet form, over multiple cycles of sulfidation and regeneration.

Table 4. Specific Sulfur Capacity of Pellets of Various Compositions Measured throughout Three Stages of Sulfidation and Regeneration

sulfidation cycle	Specific Sulfur Capacity					
	$CaCO_3$	POP1	dolime	POP2	dolomite	limestone
1	22	18.6	14.6	14.6	10	14.3
2	16.2	16.6	13.4	12.1	9.6	10.5
3	15.0	14.4	12.1	10.8	8.6	8.6

The pellets with the highest capacity were $CaCO_3$ and POP1. Since the $CaCO_3$ pellets were 99% pure, they had a relatively high specific sulfur capacity due to no inert materials. However, the $CaCO_3$ pellets did reveal a decrease in sulfur capacity (32%) almost as severe as that of the limestone pellets (40%) over the three cycles of sulfidation and regeneration. The lower capacity of the limestone pellets, with respect to the pure $CaCO_3$, was assumed to be due to the impurity content. Because both materials started off with very low surface areas, ~1.5 m^2/g, and underwent the same $CaCO_3$ decomposition, the similar drop in capacity was due primarily to the physical characteristics of the $CaCO_3$. The reason for the higher rate of sulfur capacity loss exhibited by the limestone pellets was thought to be an effect from the impurities, such as iron, acting as a fluxing agent and increasing the rate of sintering.[19] The presumed effects from the iron oxide are partially supported by observations made of the limestone pellets after the multicycle tests that revealed small, circular, brown spots on the surface of the pellets, which were thought to be iron oxide deposits consolidating on the surface. The POP1 and POP2 pellets performed similarly, with the lower, specific sulfur capacity of the POP2 pellets explained by the ~6 wt % of $MgCO_3$ within the starting material. Both types of pellets exhibited a slower decline in reactivity than the limestone and $CaCO_3$ pellets, likely due to the reasoning as stated earlier. The two forms of dolomite also showed a slower rate of deactivation than the limestone and $CaCO_3$ pellets. A surface area comparison was conducted on the materials to reveal the differences due to a lower calcination temperature. All three materials were calcined at 750 °C for 1 h in an atmosphere of flowing N_2. The dolime exhibited a postcalcination surface area of 50 m^2/g, the dolomite had a surface area of 21 m^2/g, and the limestone pellets comprised a surface area of 14 m^2/g after 1 h at 750 °C under N_2. Since the dolime and dolomite materials were composed of ~50% MgO, which was inert at the temperature tested, the extra stability exhibited by the pellets might have been due to the MgO. The reason for

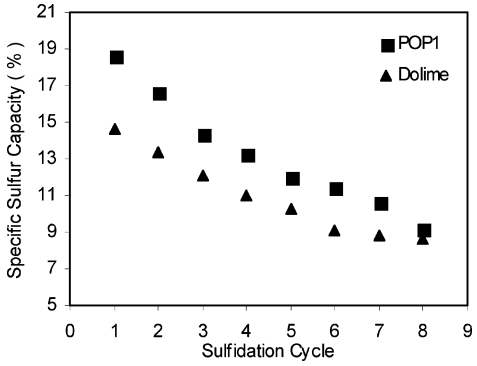

Figure 13. Single pellet comparison between POP1 and dolime pellets over consecutive sulfidation/regeneration cycles.

the higher capacity exhibited by the dolime versus dolomite is, again, probably a surface area effect. The higher surface area of the dolime is due to a chemical hydration treatment, which is similar to the treatment of calcined limestone with steam that has been reported to improve its surface area.[23] A similar comparison was shown to exist between $CaCO_3$ and $CaSO_4 \cdot 2H_2O$ previously in this paper. Of all six types of pellets compared, the pellets based upon dolomite had the lowest rate of deactiviation (14−17%/3 cycles), while the POP-based pellets were midrange with 23−26%/3 cycles, followed by the $CaCO_3$-based pellets with a 32−40%/3 cycle decline in rate.

Because the dolomite materials displayed a more constant reactivity over multiple cycles, the high concentration of MgO elicits the compound's chemically inert function during the gas−solid reactions. The reaction between calcium oxide and hydrogen sulfide (eq 2) at 880 °C exhibits a ΔH_{rxn} of −211.5 kJ/mol, and the regeneration reactions that take place at 1050 °C, which consist of the oxidation of calcium sulfide to calcium sulfate (eq 4) and the reduction of calcium sulfate to calcium oxide (eq 5), yield values of ΔH_{rxn} of −118.3 and −458.7 kJ/mol, respectively. Since the reactions are exothermic, they can potentially produce temperature gradients within the pellet, especially if it is heat transfer limited due to the fluid mechanics of the reactor. In addition to the exothermic nature of the reactions, the gas−solid reaction and solid state diffusion/reaction processes contribute to a rise in surface tension of the particles, thus increasing the driving force for sintering. Therefore, a certain amount of inert material such as MgO can have a retarding effect on the sintering rate as long as it does not act as a fluxing agent for the host material. MgO can also be described as a separating component. The separation imposed by MgO is due to the inability of the Ca^{2+} to interdiffuse within the MgO matrix because of the large differences between their atomic radii.[20] The beneficial effect exhibited by MgO has likewise been reported in studies based upon the reaction of dolomites with CO_2 at high temperatures.[21,22]

A final comparison was made between POP1 and dolime as single pellets, tested in the TGA reactor over eight cycles of suflidation/regeneration. The comparison (Figure 13) reveals that after the eighth cycle both pellets yielded similar capacities even though the POP1 pellet began with a sulfur capacity that was 22% higher than that of the dolime pellet. The stability exhibited by the hydrated dolomite is due to not only the extra porosity but also MgO. This is exemplified by these multicycle tests and indicates the importance of both attributes to a stable and reactive, high-temperature sulfur sorbent. Although the POP1 pellet does not appear to level off in its sulfur capacity, it has been shown that by 20 cycles the POP1 pellets are stable.[9] Since the dolime pellet appeared to reach a stable sulfur capacity by the eighth cycle, it would probably exceed the sulfur capacity of the POP1 pellet over more cycles. Overall, the POP1 pellet underwent a decrease in capacity of 51%/8 cycles while the dolime pellet yielded a 41%/8 cycle reduction in sulfur capacity.

Conclusions

The comparison between agglomerated pellets of limestone and plaster of Paris (POP1) for their reactivity with H_2S yielded results that were very similar in apparent density and pore size distribution, but quite contrasted with regard to physical stability. The difference in reactivity was attributed to the higher surface area of the POP1 pellets, and the physical stability was the result of the starting materials' structure. The pore-forming additive that most improved the sulfur capacity of the pelletized limestone particles over three cycles of sulfidation/regeneration was PVA, while lower performances were exhibited by the lstST and lstGR pellets. A more in-depth study on the relation between the pore-forming material and the synthesis route, including pelletization, needs to be carried out to reveal the benefits of such a process. The most promising materials, regarding sulfur capacity and stability, were the POP1 and dolime. These two pelletized materials exhibited high reactivity and relative thermal stability over eight cycles of sulfidation and regeneration. The superior stability of the dolime pellets is most likely due to surface area and pore structure of the pellets and the large fraction of MgO. In general, further improvements in CaO-based sulfur sorbents will depend upon increasing the porosity and surface area of the material while strategically incorporating materials such as MgO to thermally stabilize the sorbents for multicycle industrial uses.

Acknowledgment

This work was supported by the U.S. Department of Energy, Advanced Coal Research at U.S. Colleges and Universities Program, under Grant DE-FG26-99FT40587. Additional support was provided by Iowa State University.

Literature Cited

(1) Federal Energy Technology Center Office of Fossil Energy, U.S. DOE. Vision 21 Program Plan: Clean Energy Plants for the 21st Century. http://www.fe.doe.gov/probrams/powersystems/vision21. (accessed: Feb 10, 2003).

(2) Westmoreland, P. R.; Harrison, D. P. Evaluation of Candidate Solid for High Temperature Desulfurization of Low-Btu Gases. *Curr. Res.* **1976**, *10* (7), 659−661.

(3) Zeng, Y.; Kaytakoglu, S.; Harrison. D. P. Reduced Cerium Oxide as an Efficient and Durable High Temperature Desulfurization Sorbent. *Chem. Eng. Sci.* **2000**, *55*, 4893−4900.

(4) Jagtap, S. B.; Wheelock, T. D. Regeneration of Sulfided Calcium-Based Sorbents by a Cyclic Process. *Energy Fuels* **1996**, *10*, 821−827.

(5) Akiti, T. T.; Constant, K. P.; Doraiswamy, L. K.; Wheelock, T. D. A Regenerable Calcium-Based Core-in-Shell Sorbent for Desulfurizing Hot Coal Gas. *Ind. Eng. Chem. Res.* **2002**, *41*, 587−597.

(6) Borgwardt, R. H. Surface Area of Calcium Oxide and Kinetics of Calcium Sulfide Formation. *Environ. Prog.* **1984**, *3* (2), 129−135.

(7) Nguyen, Q. T.; Watkinson, A. P. Sulphur Capture During Gasification of Oil Sand Cokes. *Can. J. Chem. Eng.* **1993**, *71*, 401−410.

(8) Agnihotri, R.; Chauk, S. S.; Mahuli, S. K.; Fan, L. Mechanism of CaO reaction with H_2S: Diffusion through CaS product layer. *Chem. Eng. Sci.* **1999**, *54*, 3443−3453.

(9) Wheelock, T. D.; Hasler, D. J. L. A Reusable Calcium-Based Sorbent for Desulfurizing Hot Coal Gas. In *Proceedings−International Conference on Coal Science, 11th*, San Francisco, CA, Sept. 30−Oct. 5, 2001.

(10) Beruto, D.; Barco, L.; Searcy, A. W. CO_2-Catalyzed Surface Area and Porosity Changes in High-Surface-Area CaO Aggregates. *J. Am. Ceram. Soc.* **1984**, *67*, 512−515.

(11) Borgwardt, R. H. Calcium Oxide Sintering in Atmospheres Containing Water and Carbon Dioxide. *Ind. Eng. Chem. Res.* **1989**, *28*, 493−500.

(12) Borgwardt, R. H. Sintering of Nascent Calcium Oxide. *Chem. Eng. Sci.* **1989**, *44* (1), 53−60.

(13) Fuertes, A. B.; Alvarez, D.; Rubiera, F.; Pis, J. J.; Marbán, G. Surface Area and Pore Size Changes During Sintering of Calcium Oxide. *Chem. Eng. Commun.* **1991**, *109*, 73−88.

(14) Hartman, M.; Trnka, O.; Beran, Z. Kinetics of the Thermal Decomposition of Hydrated Dolomitic Lime and Sintering of Nascent Calcine. *Chem. Eng. Commun.* **1997**, *162*, 199−214.

(15) Lange, F. F. Sinterability of Agglomerated Powders. *J. Am. Ceram. Soc.* **1984**, *67* (2), 83−89.

(16) Lange, F. F. Powder Processing Science and Technology for Increased Reliability. *J. Am. Ceram. Soc.* **1989**, *72* (1), 3−15.

(17) Satterfield, C. N. *Heterogeneous Catalysis in Practice*; McGraw-Hill: St. Louis, MO, 1980.

(18) Carberry, J. J. *Chemical and Catalytic Reaction Engineering*; McGraw-Hill: St. Louis, MO, 1976.

(19) Pineda, M.; Palacios, J. M. Effect of Pore-Modifier Graphite on the Performance of a Zinc Titanate Sorbent in Hot Coal Gas Desulfurization. *Energy Fuels* **1998**, *12*, 409−415.

(20) Glasson, D. R. Reactivity of Lime and Related Oxides. XI.* Production of Dolomitic Lime. *J. Appl. Chem.* **1964**, 121−125.

(21) Van Vleck, L. H. *Elements of Materials Science and Engineering*, 3rd Edition; Addison-Wesley: Reading, MA, 1975.

(22) Bandi, A.; Specht, M.;. Sichler, P; Nicoloso, N. *In situ* Gas Conditioning in Fuel Reforming for Hydrogen Generation. Presented at the Fifth International Symposium on Gas Cleaning at High Temperatures, Sept. 17−20, 2002.

(23) Silaban, A.; Narcida, M.; Harrison, D. P. Characteristics of the Reversible Reaction Between $CO_{2(g)}$ and Calcined Dolomite. *Chem. Eng. Commun.* **1996**, *146*, 149−162.

(24) Glasson, D. R. Reactivity of Lime and Related Oxides. XII.* Hydration of Dolomitic Lime. *J. Appl. Chem.* **1964**, 125−128.

Received for review December 5, 2006
Revised manuscript received May 8, 2007
Accepted May 23, 2007

IE061561N